ADVANCED MATERIALS
www.advmat.de

A Morphable Ionic Electrode Based on Thermogel for Non-Invasive Hairy Plant Electrophysiology

Yifei Luo, Wenlong Li, Qianyu Lin, Feilong Zhang, Ke He, Dapeng Yang, Xian Jun Loh,* and Xiaodong Chen**

Plant electrophysiology lays the foundation for smart plant interrogation and intervention. However, plant trichomes with hair-like morphologies present topographical features that challenge stable and high-fidelity non-invasive electrophysiology, due to the inadequate dynamic shape adaptability of conventional electrodes. Here, this issue is overcome using a morphable ionic electrode based on a thermogel, which gradually transforms from a viscous liquid to a viscoelastic gel. This transformation enables the morphable electrode to lock into the abrupt hairy surface irregularities and establish a conformal and adhesive interface. It achieves down to one tenth of the impedance and 4–5 times the adhesive strengths of conventional hydrogel electrodes on hairy leaves. As a result of the improved electrical and mechanical robustness, the morphable electrode can record more than one order of magnitude higher signal-to-noise ratio on hairy plants and maintains high-fidelity recording despite plant movements, achieving superior performance to conventional hydrogel electrodes. The reported morphable electrode is a promising tool for hairy plant electrophysiology and may be applied to diversely textured plants for advanced sensing and modulation.

1. Introduction

Endogenous electrical signals are essential for plants' sensing and responding to the environment. Environmental stimuli such as temperature, light, and pressure can trigger widespread membrane potential variations followed by systemic alterations in gene expression, which further modulate physiological activities such as growth and fertilization.[1–5] These electrical signals are believed a fast responsive, long-distance signaling pathway, imperative to plants' survival.[1,5,6] Therefore, studying plant electrophysiology provides a solid foundation for plant interrogation and intervention through advanced electronic technology,[7–11] with potential benefits for sustainable food supply and environmental protection.

Non-invasive plant electrophysiology is preferred to invasive counterpart due to the genuineness of signals acquired without damaging plant tissues.[12] However, the uneven and irregular surface topography of plants presents a big hurdle to intimately interface with electrodes.[11] In particular, most plants develop trichomes (hair-like appendages) of diverse morphologies (straight, branched, spiral, etc.) and varying densities,[13] which can be challenging to conform and adhere to by conventional electrodes including gel electrodes. Although the use of soft and adhesive hydrogels improves contact with biological tissues,[14–17] the flat surface and well-defined geometries of pre-formed solid hydrogels hinder their conformal contact with hairy plant surfaces (**Figure 1**a-i and Figure S1: Supporting Information). Such lack of conformability will reduce adhesion force and deteriorate signal transmission stability and fidelity.[18]

On the other hand, agar gel and agar viscous solution,[19,20] applied on plants in a liquid form and connected to metal wires, may offer improved conformability. Nevertheless, they cannot accommodate plant movements due to weak adhesion (Figure 1a-ii),[21–23] thereby requiring stringent fixation and operational care to avoid electrode detachment.[12,20] In all, conventional electrodes based on hydrogel lack the adaptability to hairy topography and plant movements in dynamic testing, where conformability and adhesiveness are challenging to achieve simultaneously.

Here, we report a morphable electrode with dynamic shape adaptability to overcome the challenge and realize stable, high-fidelity signal recording on hairy plants. The morphable electrode employs thermogel as the plant-interfacing material, which is formed through in-situ gelation of a thermogelling polymer solution, where addition of salts confers conductivity. Such solution is fluidic (sol) at low temperature (≈4 °C) yet transforms

Dr. Y. Luo, W. Li, Dr. F. Zhang, Dr. K. He, Prof. X. Chen
Innovative Center for Flexible Devices (iFLEX)
Max Planck – NTU Joint Lab for Artificial Senses
School of Materials Science and Engineering
Nanyang Technological University
50 Nanyang Avenue, Singapore 639798, Singapore
E-mail: chenxd@ntu.edu.sg
Dr. Y. Luo, Q. Lin, Prof. X. J. Loh
Institute of Materials Research and Engineering
Agency for Science, Technology and Research (A*STAR)
2 Fusionopolis Way, Innovis, #08-03, Singapore 138634, Singapore
E-mail: lohxj@imre.a-star.edu.sg
Prof. D. Yang
College of Chemical Engineering and Materials Science
Quanzhou Normal University
Quanzhou, Fujian 362000, China
E-mail: yangdp@qztc.edu.cn
The ORCID identification number(s) for the author(s) of this article can be found under https://doi.org/10.1002/adma.202007848.

DOI: 10.1002/adma.202007848

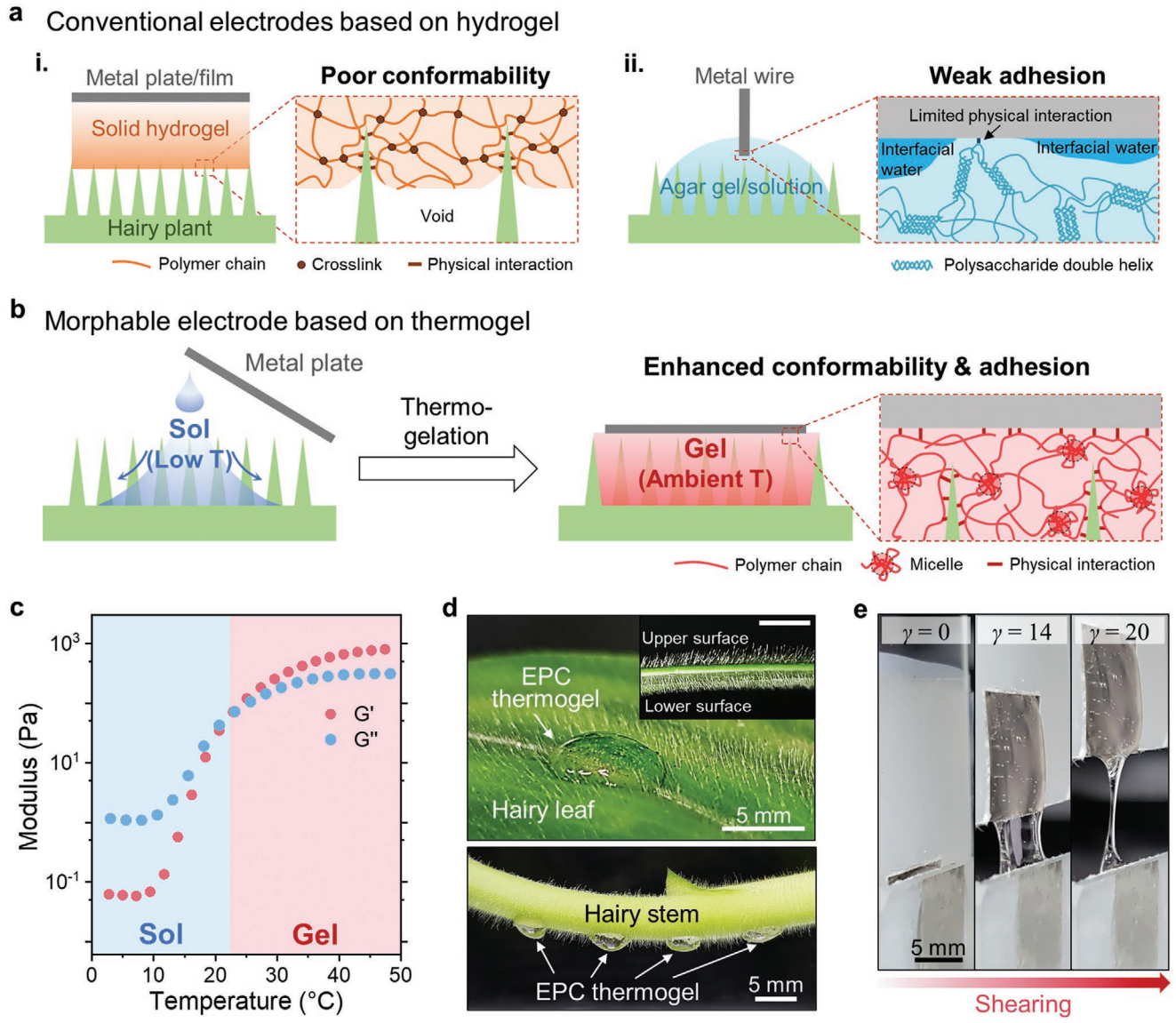

Figure 1. Overview of morphable electrode based on thermogel for conformal and adhesive interfacing with hairy plants. a) Schematics of conventional electrodes based on hydrogel when used for electrophysiology on hairy plants. i) Pre-formed solid hydrogel is not able to conform to hairy surfaces. ii) Presence of interfacial water between agar gel and solid surface causes poor adhesion. b) Schematics of applying morphable electrode on hairy plants. Cool polymer solution (sol at around 4 °C) is dropped on plant surface and solidifies into a gel as temperature equilibrates with the ambient, forming a surface electrode with enhanced conformability and adhesion. c) Rheological characterization of EPC thermogelling solution (11% EPC–0.9% NaCl w/v) at temperature ramp from 0 to 50 °C showing its sol–gel transition. Transition temperature is 22.4 °C, determined from the crossover of G' and G'' curves. d) Photographs of EPC thermogel applied on hairy plants showing its conformal contact with dense hairs and self-standing behavior when inverted. Top, *Costus productus* Gleason ex Maas (dwarf orange ginger) leaf. Inset is the side view depicting its hairy surfaces (scale bar, 5 mm). Bottom, *Nicotiana tabacum* (tobacco plant) stem. e) Photographs of EPC thermogel during shear test, demonstrating its mechanical robustness. Left: setup without stretching. Two Pt plates were kept parallel with thermogel (1 mm thick) laminated in between. Middle and right: thermogel being sheared to 14 and 20 times of its thickness, respectively. γ, shear strain.

into a viscoelastic gel at room temperature. Gentle placement of a metal plate on the thermogel completes electrode assembly (Figure 1b). We utilize the sol–gel transition to allow liquid-phase application for conformability to hairy surfaces. Meanwhile, robust adhesion stemming from polymer amphiphilicity and mobility helps to accommodate mechanical disturbances to the plant-electrode assembly. When employed for non-invasive signal measurement, morphable electrodes recorded ≈2.4 times the signal amplitude of electrodes based on solid hydrogel on hairy sunflower stems. They also recorded substantially reduced noise level and improved signal-to-noise ratio (SNR) over conventional agar-based electrodes on hairy tobacco stems when the plants were mechanically disturbed. Furthermore, the signal fidelity of non-invasive morphable electrodes even approached invasive measurements. These results demonstrate the superiority of our morphable electrodes for hairy plant electrophysiology.

2. Results and Discussion

The thermogelling polymer we used is a multi-block amphiphilic copolymer previously developed in our lab.[24,25] It consists of hydrophilic poly(ethylene glycol) (PEG), thermoresponsive poly(propylene glycol) (PPG), and hydrophobic biodegradable polycaprolactone (PCL) segments, named poly(PEG/PPG/PCL urethane) and denoted as EPC (molecular structure and chemical characterizations provided in Figures S2–S4 and Table S1, Supporting Information). Upon temperature increase, dehydration of PPG segments drives the formation of a supramolecular hydrogel matrix in an associated micellar structure (Figure 1b, right).[26] EPC thermogel was previously used as a vitreous tamponade in the eye,[25] assuring biocompatibility on plants. The thermogelling solutions showed large yet gradual rheological change upon sol–gel transition,[25] desirable for the practical implementation of in-situ gelated electrodes. The low critical gelation concentration (3 wt%) can boost ionic conductivity and transition temperatures (20–40 °C) near ambient temperatures are suitable for plant-targeted applications.[24] The flexible and amphiphilic EPC polymer could promote wetting on hydrophobic plant surfaces,[27,28] favorable for conformal and adhesive contact. Additionally, the viscosity, storage and loss moduli, sol–gel transition temperature, and gelation time can be easily tuned through polymer and salt concentrations (Figures S5 and S6, Supporting Information),[29] giving us freedom in designing thermogels with optimal properties according to application conditions. The optimized thermogelling solution (11% EPC-0.9% NaCl w/v) shows a sol–gel transition at 22.4 °C, and more than three orders of magnitude increase in storage modulus from 4 to 25 °C (Figure 1c). Applying the solution to hairy plants gives liquid-like contact, yet enough adhesiveness and cohesiveness to hold its own weight after gelation (Figure 1d) and even withstand >1000% shear strain (Figure 1e) (Movies S1 and S2, Supporting Information).

To verify the design concept of sol–gel transition-enabled conformability, we first compare the rheological properties of the EPC thermogelling solution (EPC_TGS) with agar gelling solution (agar_GS, homogeneous solution), agar viscous solution (agar_VS, dispersion of gel particles[23]), and chemically crosslinked polyacrylamide (PAAm) hydrogel (a representative solid hydrogel), in response to temperature change (**Figure 2**a,b) (preparation of gels/solutions described in experimental details, Supporting Information). Designed to be a sol at low temperatures and a gel at elevated temperatures, EPC_TGS attains the lowest viscosity and the highest tanδ at 0–10 °C across the temperature range. This trend is opposite to the behavior of agar, which dissolves in hot water and solidifies at below ≈40 °C (agar_GS).[21] In contrast, both agar_VS and PAAm hydrogel show no obvious rheological change with temperature, due to pre-formed gel structures. Rheological properties of gels/solutions when applied on plants critically determine their interaction with plants; thus we compare the viscosity and tanδ at the application temperatures of various gels/solutions (Figure 2c,d). EPC_TGS has the second lowest viscosity (≈220 mPa s at 5 °C) and the highest tanδ (≈18 at 5 °C) among all gels/solutions, suggesting high sol fluidity and chain mobility when applied on plants, beneficial for filling surface roughness and thus enhancing conformability and interfacial adhesion.[30,31]

We then confirmed the surface activity of EPC polymers through surface tension and contact angle measurements. For instance, only 0.1% w/v EPC added can reduce the surface tension of a saline droplet in air from 71 to 49 mN m^{-1} (Figure S7, Supporting Information). Moreover, sessile drops of 0.03% w/v EPC solution have significantly smaller contact angles on synthetic polymers and fresh leaves than pure saline, and larger contact angles on metal-based conductors (Figure 2e), implying changes in liquid–solid interfacial energy caused by physical adsorption of EPC polymers, which may enhance the interaction between thermogel network and adherent surfaces (Note S1, Supporting Information). The improved wetting on hydrophobic surfaces tackles the waxy cuticle on plants[32,33] and can promote conformal contact when the surface is rough.[27,28,34] In contrast to EPC polymers, minimal changes in surface tension (Figure S7, Supporting Information) and contact angle (Figure 2e) were observed when adding agar polymers to saline.

With the understanding of sol fluidity, chain mobility, and surface activity, we then visualized the degree of conformability of EPC thermogel on hairy plants using cross-sectional scanning electron microscopy (SEM). Figure 2f reveals seamless contact between EPC thermogel and a hairy leaf with well-preserved hair morphology, and the magnified image in Figure S8 (Supporting Information) depicts a hair wrapped tightly with EPC polymers, showing direct contact between polymer and plant, in accordance with the hypothesis of interfacial adsorption. As for agar gel (formed in situ from agar gelling solution), tiny slits (≈37 μm wide, Figure 2g) present at the interface, possibly because freeze-drying during sample preparation induced interfacial detachment due to differential thermal expansion/contraction. For PAAm hydrogel, large gaps (≈270 μm wide) separate the gel and the leaf, with some trichomes damaged and some piercing the hydrogel. Based on these results, we conclude that EPC thermogel can establish a conformal interface with hairy leaves while preserving the intactness of vulnerable trichomes.

Serving as a bridge between plants and metal conductors, the thermogel should be both mechanically and electrically robust. Thus, we first quantitatively study the adhesive properties of EPC thermogel. Using lap-shear tests (Figure S9, Supporting Information),[35] we measured the adhesive strengths of EPC thermogel on Ag/AgCl plates and hairy leaves of gloxinia (*Sinningia speciosa*) respectively, agar gel and PAAm hydrogel being controls. Both agar gel and EPC thermogel were applied in sol state to attain maximal adhesive strengths (Figure S10, Supporting Information). As summarized in **Figure 3**a, EPC thermogel fails cohesively (i.e., inside gel bulk) with a strength around 170–180 Pa, regardless of adherends. This implies robust interfacial bonding such that the bulk gel strength becomes the limiting factor in shear adhesion. This feature of cohesive failure will help preserve plant tissues during electrode detachment. In addition, the not dissimilar behavior on hairy plants and metal plates underscores the versatility of amphiphilic polymers in establishing physical contact with surfaces of distinct chemistry, concurring with previous results on the adsorption of poly(ethylene oxide) (PEO)- and poly(propylene oxide) (PPO)-based block copolymers.[36,37] Conversely, agar gel and PAAm hydrogel tend to fail adhesively (i.e., at interface). Agar gel adheres very weakly on Ag/AgCl (34 Pa),

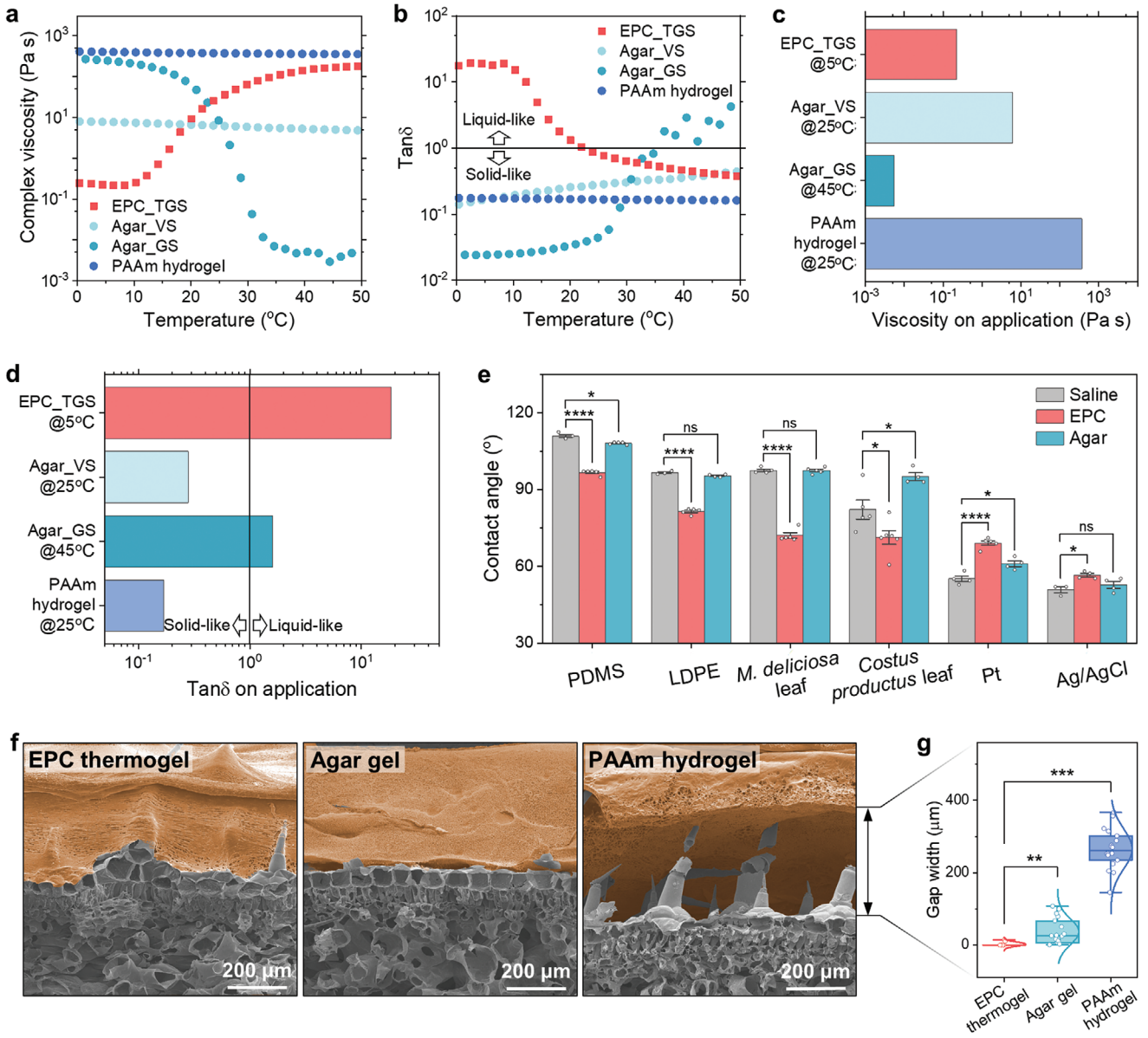

Figure 2. Fluidic characteristics of EPC solution and its conformal contact with hairy plants. a,b) Viscosity (a) and tanδ (G''/G') (b) in the range of 0–50 °C of 11% EPC thermogelling solution (EPC_TGS), 0.5% agar viscous solution (agar_VS), 0.5% agar gelling solution (agar_GS), and 11% w/v PAAm hydrogel. c,d) Comparison of viscosity (c) and tanδ (d) at the respective application temperature of various gels and solutions, showing low viscosity and large liquid character of EPC sol, beneficial for conformal contact. e) Histogram showing contact angles of sessile drops of saline, EPC solution, and agar solution (polymer concentration of 0.03% w/v) on various surfaces (mean ± s.e.), revealing strong surface activity of EPC polymer, which could contribute to conformal and adhesive contact. *$p < 0.05$, ****$p < 0.0001$; unpaired, two-tailed t-test. ns, not significant. f) Cross-sectional scanning electron microscopy images of gels applied on gloxinia (*Sinningia speciosa*) leaves depicting a high degree of conformability of EPC thermogel. Orange shading outlines the gels, and gray regions are plant tissues. g) Box plot of gap widths between leaf surfaces and gels (median, 25th and 75th percentiles, minimum and maximum; $n = 9$ for EPC thermogel, $n = 18$ for agar gel and PAAm hydrogel). **$p < 0.01$, ***$p < 0.001$; unpaired, two-tailed t-test.

which is presumably due to low polymer mass ratio, lack of surface activity, and syneresis (extruding water on standing,[21] Figure S11, Supporting Information), whereas PAAm hydrogel adheres weakly on hairy leaves (48 Pa), indicating the prominent effect of poor contact due to presence of hairs.[38]

The adhesive properties of electrodes based on different hydrogels were then compared in shear tests on tobacco (*Nicotiana benthamiana*) stems, where stems in pots were fixed while electrodes were pulled vertically upward (Figure 3b). Inferred from lap-shear testing results, EPC-thermogel-based electrodes should fail cohesively with the largest shear strength whereas agar-gel- and PAAm-hydrogel-based electrodes should fail adhesively. The load–displacement curves in Figure 3c confirm the largest shear strength of EPC thermogel-based electrodes (15 mN peak load for EPC thermogel vs 4.0 mN for agar gel and 1.8 mN for PAAm hydrogel), and photographs

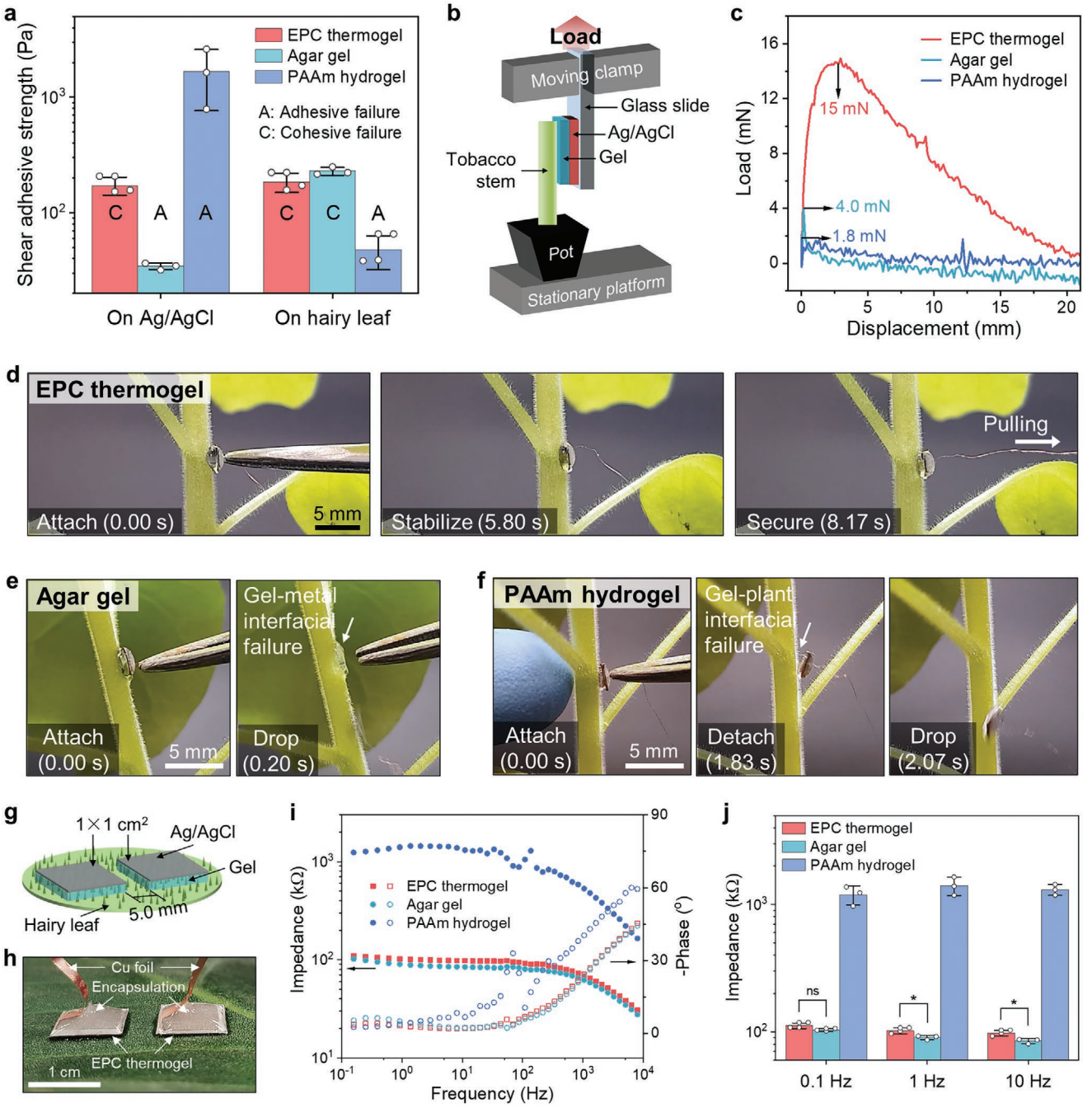

Figure 3. Adhesive and electrical properties of EPC thermogel. a) Histogram showing shear adhesive strengths of EPC thermogel, agar gel, and PAAm hydrogel on Ag/AgCl plates and hairy leaves of gloxinia (mean ± s.d.). EPC thermogel fails cohesively regardless of substrates, implying robust interfacial adhesion. b) Schematic of the experimental setup for shear tests of gel-based electrodes on tobacco (*Nicotiana benthamiana*) stems. c) Representative load–displacement curves from the shear tests, showing substantially higher shear force of EPC thermogel-based electrodes than controls. Load is not converted to stress due to difficulty in accurately measuring contact area (roughly controlled at 1 cm^2). d–f) Snapshots of applying plate electrodes based on different hydrogels (electrode construction shown in Figure S12, Supporting Information) on tobacco stems. Only did EPC thermogel secure the electrode firmly. g,h) Schematic (g) and photograph (h) showing the setup for measuring impedance of gel-based electrodes on hairy leaves. i) Mean impedance and phase angle of various gel-based electrodes ($n = 3$) on hairy leaves. j) Histogram comparing the impedance of gel-based electrodes on hairy leaves at three frequencies relevant to plant electrophysiology in this study. The comparable impedance of EPC thermogel to agar gel proves effective gel-leaf electrical contact, outperforming PAAm hydrogel. $^*p < 0.05$; unpaired, two-tailed *t*-test. ns, not significant.

of samples during shearing show failure modes as predicted (Figure S12a, Supporting Information). We also did a series of shear oscillation tests to characterize the cohesive mechanical properties of different gels and observed in EPC thermogel outstanding deformability (220% yield strain, vs 23% for agar gel and 39% for PAAm hydrogel) and good strength (580 Pa

yield strength, vs 180 Pa for agar gel and 640 Pa for PAAm hydrogel) (Figure S13, Supporting Information), which contribute to the dynamic adaptability of EPC thermogel during plant movements. As a result of strong adhesion and cohesion, EPC thermogel secured plate electrodes (schematic shown in Figure S14, Supporting Information) firmly on tobacco stems and could withstand gentle pulling (Figure 3d and Movie S3: Supporting Information), whereas agar gel and PAAm hydrogel could not even adhere the electrodes on stems (Figure 3e,f and Movies S4 and S5: Supporting Information).

Next, we fully characterized the electrical properties of the electrode based on thermogel as follows. First, we measured the intrinsic conductivity of EPC thermogel, which is comparable to PAAm hydrogel at the same polymer mass ratio (Figure S15, Supporting Information). We then measured the impedance of gel-metal conductor (Ag/AgCl and Pt) laminates (Figure S16, Supporting Information), where EPC thermogel possessed similar values to control gels. Next, we compared the impedance of gel-based electrodes on hairy leaves (Figure 3g,h). The comparable impedance of electrodes based on EPC thermogel and agar gel (Figure 3i,j) indicates similarly conformal contact, whereas the more than one order of magnitude higher impedance of PAAm hydrogel-based electrodes (e.g., 1.2 MΩ for PAAm hydrogel vs 0.11 MΩ for EPC thermogel at 0.1 Hz) should be attributed to poor gel-leaf contact. We further verified on a control plant with only sparse trichomes (*Arabidopsis thaliana*), that the quality of electrical coupling between EPC thermogel and plants does not deviate from agar gel and PAAm hydrogel (Figure S17, Supporting Information). These results prove that EPC thermogel is an effective electrical bridge on hairy plants due to adequate conductivity and conformability.

To demonstrate the superiority of morphable electrodes based on thermogel for non-invasive electrophysiology on hairy plants, we recorded flame-induced potential variations on hairy sunflower and tobacco stems using electrodes in pairs, one of which was the morphable electrode and the other was a control electrode, in a setup shown in **Figure 4**a (exact electrode positions in Figure S18, Supporting Information). Unlike previous studies where the metal conductors must be precisely secured by external fixtures,[12,39,40] we constructed Ag/AgCl plates with Cu wiring (Figure S14, Supporting Information), which allows for facile and versatile placement on plants with great operational simplification and spatial freedom. Due to the poor adhesion between agar gel and Ag/AgCl plates, measurement using agar gel in such electrode configuration was not successful (Figure 3e and Movie S4: Supporting Information). Instead, we used the conventional agar-wire construction where the Ag/AgCl wire is secured by a manipulator.[12]

We first compared the signal quality of electrodes based on EPC thermogel and PAAm hydrogel on sunflower stems. As seen in Figure 4b, PAAm hydrogel could barely adhere on hairs leaving obvious gaps, whereas EPC thermogel conformally anchored Ag/AgCl plates on sunflower stems. Flame wounding of a leaf tip induced a series of potential variations in the stem,[39] and EPC thermogel and PAAm hydrogel in a pair captured synchronized signals (Figure S19a, Supporting Information). The recorded potentials display large depolarizations upon wounding in a range of 41–73 mV with signal transmission speed within 7.8–23 cm min^{-1}, consistent with previous reports.[39,41] Analysis of signal amplitude shows that EPC thermogel records significantly (P = 0.014) higher intensity than PAAm hydrogel (Figure 4c), believed a result of more conformal contact by the former. Moreover, the superiority of EPC thermogel seems to be more prominent for peaks with amplitude below 40 mV, where the signal intensity is ≈2.4 times that of PAAm hydrogel (Figure S19b,c, Supporting Information).

We further challenged morphable electrodes by conducting the flame-wounding experiment on tobacco plants, whose stem hair density is much higher than that of sunflowers and even prevented adhesion of PAAm hydrogel (Figure 3f and Movie S5: Supporting Information). Nevertheless, morphable electrodes could still adhere reliably on such densely hairy surfaces (Figure 3d and Movie S3, Figure S20: Supporting Information). To prove the importance of reliable mechanical bridging to signal stability, we recorded signals using morphable electrodes and agar-wire electrodes while manually touching the plants or with wind blowing (Figure 4d,e and Movie S6, Figures S21 and S22: Supporting Information). In these experiments, morphable electrodes could maintain a stable signal baseline with minimal noise, but agar-based electrodes either recorded obvious fluctuations or large drifts, as a result of detachment between agar gels and Ag/AgCl wires when the plants experienced movements (Figure 4d and Movie S7: Supporting Information). Subsequently, wound-induced depolarizations were not as effectively recorded as by morphable electrodes. Statistical analysis of five repetitions of the above experiment (Table S2, Supporting Information) gives a background noise level of 0.084 ± 0.010 mV and an SNR of 47 ± 5.0 dB for morphable electrode, and 0.12 ± 0.041 mV and 43 ± 3.6 dB respectively for agar-wire electrode. These results validate the vital role of the robust mechanical interface established by morphable electrodes.

Finally, we benchmarked the signal quality of morphable electrodes against that of inserted Ag/AgCl wires, a standard invasive method,[12,39] on tobacco plants (Figure 4f,g). In a typical test shown in Figure 4g, potential was recorded using the Ag/AgCl wire during the application of a morphable electrode (purple shading), and the small transient peaks indicate minimal interference to plant electrophysiology induced by solution coolness and gentle pressure. Following flame-wounding an upper leaf, depolarization up to 35 mV was recorded from the morphable electrode, approaching 37 mV from the inserted Ag/AgCl wire (26 ± 9.9 and 27 ± 9.4 mV respectively from three independent tests, SNRs being comparable as well, Figure 4g inset). This comparable signal quality is supported by the similar impedance of the two types of electrodes on tobacco stems (Figure S23, Supporting Information). We also showed morphable electrodes could monitor signal transmission within tobacco stems (Figure S24, Supporting Information), and the signal amplitude and duration generally match those reported in a similar study (more details in Note S3, Supporting Information).[42] In all, these plant electrophysiological measurements demonstrate that morphable electrodes can record clearer and more stable signals than solid hydrogel- and agar-based electrodes on hairy plants; being almost imperceptible to plants, the morphable electrodes are competitively capable of faithful recording as invasive measurement, being an effective tool for plant electrophysiology.

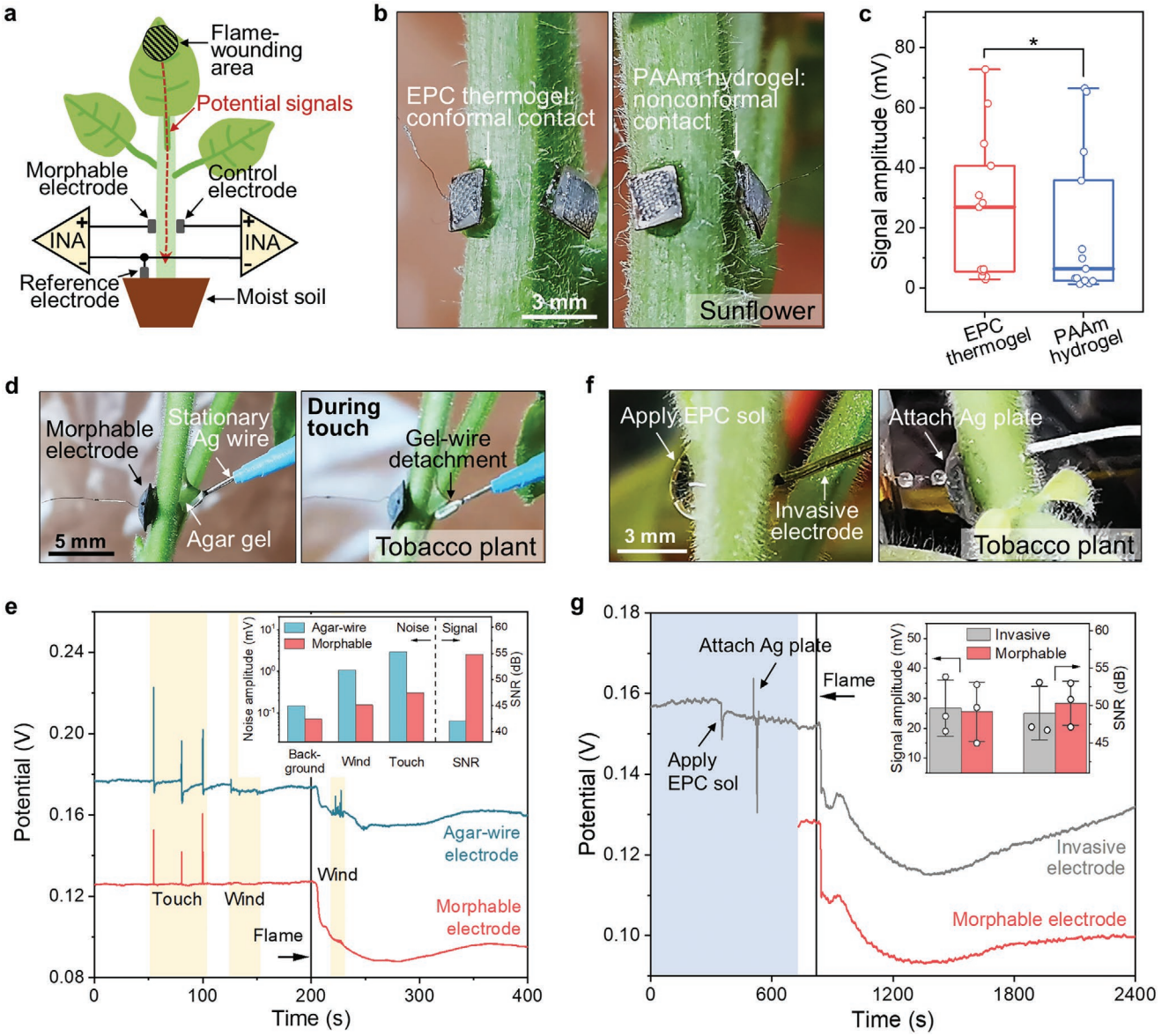

Figure 4. Non-invasive monitoring of wound-induced potential signals in hairy plants by morphable electrodes. a) Schematic showing the setup for the wounding experiments. INA, instrumentation amplifier. b) Photographs showing plate electrodes adhered on a hairy sunflower stem through EPC thermogel and PAAm hydrogel, respectively, depicting contrasting conformability of the two gels. c) Box plot of signal amplitudes read from EPC thermogel and PAAm hydrogel on sunflower stems (median, 25th and 75th percentiles, minimum and maximum, $n = 13$ from 5 plants), implying higher signal intensity from EPC thermogel. $^*p < 0.05$; paired t-tests. d) Photographs of morphable electrode and agar gel–Ag/AgCl wire electrode reading signals on tobacco stems. Agar gel easily detached from Ag/AgCl wire when the plant was touched while morphable electrode maintained stable connection (right). e) Signals from the electrodes in d in a flame-wounding experiment. Yellow shading indicates intervals of mechanical disturbance. Inset displays quantified comparison of signal quality between the two electrodes (root mean square (rms) background noise amplitude, rms wind noise amplitude, mean baseline shift due to touch ($n = 3$), wounding signal to background noise ratio (SNR), detailed data analysis method provided in experimental details, Supporting Information). Morphable electrode reads more stable and clearer signals due to robust adhesion. f) Photographs showing the attachment of morphable electrode during benchmarking against inserted Ag/AgCl wire. g) Signals read from invasive Ag/AgCl wire and morphable electrode in a flame-wounding test. Purple shading indicates the period of morphable electrode attachment. Inset displays comparable signal quality of morphable electrode and invasive electrode in three independent experiments (mean ± s.d.).

An adhesive and conformal bio-electronic interface is essential in wearable sensing devices for reliable signal acquisition in dynamic environments,[18] which has seen fast progress in skin and tissue-mountable sensors[43–45] but the counterpart on plants is much less explored.[11,17] In this work, we addressed the issue of interfacing with hairy plants, one of the most challenging topographies to tackle. This expands the library of plant species and plant parts accessible for non-invasive monitoring. The robust mechanical interface established by morphable electrode allows us to nullify the cumbersome electrode fixtures and to record stable signals even under mechanical disturbances, a promising attempt toward "plant

wearable sensors". Additionally, with proper encapsulation, our morphable electrode can realize long-term monitoring for at least 4 days (Figure S25, Supporting Information). Future work will be developing electrodes that can accommodate plant growth for longer periods of monitoring and fast-growing seedlings. Our work sets the scene for future device development toward smart plant monitoring and modulation, which will find wide applications in environmental sensing,[7] crop health monitoring,[11] plant physiology regulation and modification,[9,11,46–48] and augmented human-plant interaction.[8,10]

Using hairy plants as a model system, we proved the efficacy of morphable materials that involve liquid-to-solid (or semisolid) transition in bridging textured biological tissues. Recent development of soft materials for bioelectronics largely leverages modulus and thickness reduction for improved conformability.[49,50] Here we extend the lower modulus limit to liquid regime to tackle the most abruptly irregular surfaces including high-aspect-ratio topographies, which may provide inspirations for conformal electronics on other intricately textured biological tissues such as the brain. In addition, endowing morphable materials with properties other than electrical conductivity will realize more sensing capabilities beyond electrophysiology. We envision such morphable ionic electrodes based on responsive polymers, utilizing the unique properties of soft materials, will stimulate broader integration between biology and electronics through smart material design.[51,52]

3. Conclusion

We have demonstrated a morphable ionic electrode based on a thermogel, which utilizes the in situ sol–gel transition of an amphiphilic flexible polymer and can establish an adhesive and conformal, mechanical, and electrical interface on hairy plants, realizing high-fidelity electrophysiological recording not achievable by conventional gel-based electrodes. Our morphable electrode provides not only a useful toolkit for fundamental plant studies but also an effective solution to plant–electronic hybridization, generating inspirations for soft-material-incorporating bioelectronics.

4. Experimental Section

Experimental details are provided in the Supporting Information.

Supporting Information

Supporting Information is available from the Wiley Online Library or from the author.

Acknowledgements

The authors thank the financial support from the Agency for Science, Technology and Research under its AME Programmatic Funding Scheme (A18A1b0045), the National Research Foundation, Prime Minister's Office, Singapore, under its NRF Investigatorship (NRF-NRFI2017-07), and Singapore Ministry of Education (MOE2019-T2-2-022). The authors appreciate the initial provision of polymers and project advice by Dr. Sing Shy Liow, and suggestions on improving the work from Dr. Liang Pan and Dr. Shaobo Ji.

Conflict of Interest

The authors declare no conflict of interest.

Data Availability Statement

The main data supporting the findings of this study are available within the article and its Supporting Information files. Extra data are available from the corresponding authors upon reasonable request.

Keywords

bioelectronics, conformal electrodes, plant electrophysiology, supramolecular hydrogels, thermogelling polymers

Received: November 18, 2020
Revised: January 9, 2021
Published online:

[1] E. Davies, in *Plant Electrophysiology: Theory and Methods*, (Ed: A. G. Volkov), Springer, Berlin/Heidelberg, Germany **2006**, pp. 407–422.
[2] D. C. Wildon, J. F. Thain, P. E. H. Minchin, I. R. Gubb, A. J. Reilly, Y. D. Skipper, H. M. Doherty, P. J. O'Donnell, D. J. Bowles, *Nature* **1992**, *360*, 62.
[3] B. Stanković, E. Davies, *FEBS Lett.* **1996**, *390*, 275.
[4] B. Stanković, E. Davies, *Plant Cell Physiol.* **1998**, *39*, 268.
[5] E. Król, H. Dziubińska, K. Trębacz, in *Action Potential: Biophysical and Cellular Context, Initiation, Phases, and Propagation*, (Ed: M. L. DuBois), Nova Science, New York **2010**, Ch. 1, pp. 1–26.
[6] W. G. Choi, R. Hilleary, S. J. Swanson, S. H. Kim, S. Gilroy, *Annu. Rev. Plant Biol.* **2016**, *67*, 287.
[7] H. Sareen, P. Maes, in *CHI EA '19: Extended Abstracts of the 2019 CHI Conf. on Human Factors in Computing Systems* **2019**, LBW0237; https://doi.org/10.1145/3290607.3313091.
[8] S. Kuribayashi, Y. Sakamoto, H. Tanaka, in *CHI EA '07: CHI '07 Extended Abstracts on Human Factors in Computing Systems*, ACM, New York **2007**, pp. 2537–2542; https://doi.org/10.1145/1240866.1241037.
[9] E. Stavrinidou, R. Gabrielsson, E. Gomez, X. Crispin, O. Nilsson, D. T. Simon, M. Berggren, *Sci. Adv.* **2015**, *1*, 1501136.
[10] L. Angelini, M. Caon, S. Caparrotta, O. A. Khaled, E. Mugellini, in *UbiComp '16: Proc. 2016 ACM Int. Joint Conf. on Pervasive and Ubiquitous Computing: Adjunct*, ACM, New York **2016**, pp. 1001–1009; https://doi.org/10.1145/2968219.2968266.
[11] J. J. Kim, L. K. Allison, T. L. Andrew, *Sci. Adv.* **2019**, *5*, eaaw0463.
[12] S. A. Mousavi, C. T. Nguyen, E. E. Farmer, S. Kellenberger, *Nat. Protoc.* **2014**, *9*, 1997.
[13] P. Dalin, J. Ågren, C. Björkman, P. Huttunen, K. Kärkkäinen, in *Induced Plant Resistance to Herbivory*, (Ed: A. Schaller), Springer, Dordrecht, The Netherlands **2008**, pp. 89–105.
[14] L. Pan, P. Cai, L. Mei, Y. Cheng, Y. Zeng, M. Wang, T. Wang, Y. Jiang, B. Ji, D. Li, X. Chen, *Adv. Mater.* **2020**, *32*, 2003723.
[15] P. Cai, C. Wan, L. Pan, N. Matsuhisa, K. He, Z. Cui, W. Zhang, C. Li, J. Wang, J. Yu, M. Wang, Y. Jiang, G. Chen, X. Chen, *Nat. Commun.* **2020**, *11*, 2183.

[16] C. Xie, X. Wang, H. He, Y. Ding, X. Lu, *Adv. Funct. Mater.* **2020**, *30*, 1909954.
[17] W. Li, N. Matsuhisa, Z. Liu, M. Wang, Y. Luo, P. Cai, G. Chen, F. Zhang, C. Li, Z. Liu, Z. Lv, W. Zhang, X. Chen, *Nat. Electron.* **2021**, *4*, 134.
[18] T. Wang, M. Wang, L. Yang, Z. Li, X. J. Loh, X. Chen, *Adv. Mater.* **2020**, *32*, 1905522.
[19] R. Stahlberg, R. E. Cleland, E. Van Volkenburgh, *Planta* **2005**, *220*, 550.
[20] S. A. Mousavi, A. Chauvin, F. Pascaud, S. Kellenberger, E. E. Farmer, *Nature* **2013**, *500*, 422.
[21] T. Divoux, B. Mao, P. Snabre, *Soft Matter* **2015**, *11*, 3677.
[22] B. Saint-Michel, T. Gibaud, M. Leocmach, S. Manneville, *Phys. Rev. Appl.* **2016**, *5*, 034014.
[23] I. T. Norton, D. A. Jarvis, T. J. Foster, *Int. J. Biol. Macromol.* **1999**, *26*, 255.
[24] X. J. Loh, B. J. Yee, F. S. Chia, *J. Biomed. Mater. Res., Part A* **2012**, *100*, 2686.
[25] Z. Liu, S. S. Liow, S. L. Lai, A. Alli-Shaik, G. E. Holder, B. H. Parikh, S. Krishnakumar, Z. Li, M. J. Tan, J. Gunaratne, V. A. Barathi, W. Hunziker, R. Lakshminarayanan, C. W. T. Tan, C. K. Chee, P. Zhao, G. Lingam, X. J. Loh, X. Su, *Nat. Biomed. Eng.* **2019**, *3*, 598.
[26] X. J. Loh, S. H. Goh, J. Li, *Biomacromolecules* **2007**, *8*, 585.
[27] M. Song, J. Ju, S. Luo, Y. Han, Z. Dong, Y. Wang, Z. Gu, L. Zhang, R. Hao, L. Jiang, *Sci. Adv.* **2017**, *3*, 1602188.
[28] M. Song, D. Hu, X. Zheng, L. Wang, Z. Yu, W. An, R. Na, C. Li, N. Li, Z. Lu, Z. Dong, Y. Wang, L. Jiang, *ACS Nano* **2019**, *13*, 7966.
[29] S. S. Liow, Q. Dou, D. Kai, A. A. Karim, K. Zhang, F. Xu, X. J. Loh, *ACS Biomater. Sci. Eng.* **2016**, *2*, 295.
[30] J. N. Israelachvili, in *Intermolecular and Surface Forces*, 3rd ed., (Ed: J. N. Israelachvili), Academic Press, San Diego, CA, USA **2011**, pp. 415–467.
[31] H. J. Kim, K. Jin, J. Shim, W. Dean, M. A. Hillmyer, C. J. Ellison, *ACS Sustainable Chem. Eng.* **2020**, *8*, 12036.
[32] C. Müller, in *Induced Plant Resistance to Herbivory*, (Ed: A. Schaller), Springer, Dordrecht, The Netherlands **2008**, pp. 107–129.
[33] D. Hegebarth, C. Buschhaus, M. Wu, D. Bird, R. Jetter, *Plant J.* **2016**, *88*, 762.
[34] L. Barbieri, E. Wagner, P. Hoffmann, *Langmuir* **2007**, *23*, 1723.
[35] H. Yuk, C. E. Varela, C. S. Nabzdyk, X. Mao, R. F. Padera, E. T. Roche, X. Zhao, *Nature* **2019**, *575*, 169.
[36] T. J. Barnes, C. A. Prestidge, *Langmuir* **2000**, *16*, 4116.
[37] W. Hellmich, J. Regtmeier, T. T. Duong, R. Ros, D. Anselmetti, A. Ros, *Langmuir* **2005**, *21*, 7551.
[38] H. Zahouani, M. E.l Mansori, in *Characterisation of Areal Surface Texture*, (Ed: R. Leach), Springer, Berlin/Heidelberg, Germany **2013**, pp. 217–267.
[39] B. Stanković, D. L. Witters, T. Zawadzki, E. Davies, *Physiol. Plant.* **1998**, *103*, 51.
[40] H. H. Felle, M. R. Zimmermann, *Planta* **2007**, *226*, 203.
[41] B. Stankovic, T. Zawadzki, E. Davies, *Plant Physiol.* **1997**, *115*, 1083.
[42] M. Senavirathna, T. Asaeda, *Plant Signaling Behav.* **2018**, *13*, 1486145.
[43] S. Baik, H. J. Lee, D. W. Kim, J. W. Kim, Y. Lee, C. Pang, *Adv. Mater.* **2019**, *31*, 1803309.
[44] Y. Gao, L. Yu, J. C. Yeo, C. T. Lim, *Adv. Mater.* **2020**, *32*, 1902133.
[45] J. Deng, H. Yuk, J. Wu, C. E. Varela, X. Chen, E. T. Roche, C. F. Guo, X. Zhao, *Nat. Mater.* **2020**, *20*, 229.
[46] H. Sareen, J. Zheng, P. Maes, in *CHI EA '19: Extended Abstracts of the 2019 CHI Conf. on Human Factors in Computing Systems*, ACM, New York **2019**, VS13; https://doi.org/10.1145/3290607.3311778.
[47] Y. Lu, K. Xu, L. Zhang, M. Deguchi, H. Shishido, T. Arie, R. Pan, A. Hayashi, L. Shen, S. Akita, K. Takei, *ACS Nano* **2020**, *14*, 10966.
[48] F. Zhao, J. He, X. Li, Y. Bai, Y. Ying, J. Ping, *Biosens. Bioelectron.* **2020**, *170*, 112636.
[49] J. W. Jeong, W. H. Yeo, A. Akhtar, J. J. Norton, Y. J. Kwack, S. Li, S. Y. Jung, Y. Su, W. Lee, J. Xia, H. Cheng, Y. Huang, W. S. Choi, T. Bretl, J. A. Rogers, *Adv. Mater.* **2013**, *25*, 6839.
[50] G. Chen, N. Matsuhisa, Z. Liu, D. Qi, P. Cai, Y. Jiang, C. Wan, Y. Cui, W. R. Leow, Z. Liu, S. Gong, K.-Q. Zhang, Y. Cheng, X. Chen, *Adv. Mater.* **2018**, *30*, 1800129.
[51] H. Yuk, B. Lu, X. Zhao, *Chem. Soc. Rev.* **2019**, *48*, 1642.
[52] C. Yang, Z. Suo, *Nat. Rev. Mater.* **2018**, *3*, 125.